Journal of Surface Analysis Vol.15, No. 2 (2008) pp. 150−158
T. Nagatomi et al. Inelastic Interaction of Medium-Energy Electrons with Ni Surface Studied by Absolute Reflection Electron Energy Loss Spectrum Analysis and Monte Carlo Simulation

Review

Inelastic Interaction of Medium-Energy Electrons with Ni Surface Studied by Absolute Reflection Electron Energy Loss Spectrum Analysis and Monte Carlo Simulation

T. Nagatomi[a,*] and K. Goto[b]
[a]*Department of Material and Life Science, Graduate School of Engineering, Osaka University Suita, Osaka 565-0871, Japan*
[b]*National Institute of Advanced Industrial Science and Technology (AIST) Chubu, Moriyama-ku, Nagoya, Aichi 463-8560, Japan*
[*]*nagatomi@mls.eng.osaka-u.ac.jp*

(Received: February 15, 2008; Accepted: April 22, 2008)

The results of the investigation of the inelastic interaction of medium-energy electrons with the Ni surface were described. The inelastic mean free path (IMFP), the surface excitation parameter (SEP) and the differential SEP (DSEP) were deduced simultaneously from an absolute reflection electron energy loss spectroscopy (REELS) spectrum. The present IMFPs show a good agreement with those calculated using the TPP-2M predictive equation. The dependence of the SEPs on the electron energy is similar to that calculated using Werner's and Gertgely's predictive equations. The DSEPs show a reasonable agreement with the theoretical DSEPs calculated using Tung's theory with optical data. The derived IMFP, SEP and DSEP were applied to Monte Carlo simulation of REELS spectra, in which energy loss processes of signal electrons due to surface excitations were taken into account. The simulated REELS spectra reproduce the experimental absolute REELS spectra well without any fitting parameters, indicating that surface excitations play an important role in the inelastic interaction of medium-energy electrons with the solid surface.

1. Introduction

Quantitative information on the inelastic interaction of electrons with the solid surface has been important issue for quantitative surface chemical analysis by means of X-ray photoelectron spectroscopy (XPS), Auger electron spectroscopy (AES) and reflection electron energy loss spectroscopy (REELS). The inelastic mean free path (IMFP) is one of the most important parameters for quantification, which describes the decay of the peak intensity by inelastic interactions in solids. Recently, surface excitations have been proven to play an important role in inelastic interactions between electrons and solid surfaces. Surface excitations also cause the decay of the intensity of signal electrons during their transport in solids. The decay due to surface excitation is usually described by the surface excitation parameter (SEP) [1,2].

The interaction of electrons with the solid surface has been intensively studied, and the determination of parameters such as the IMFP and SEP has been performed using experimental and theoretical approaches. One of the most widely used experimental approaches for such studies is the elastic peak electron spectroscopy (EPES) analysis [1,3-6]. Another experimental approach is the REELS analysis [7-13]. Both experimental approaches are found to be effective for determining IMFP and SEP.

The EPES analysis requires a reference material and the IMFP or SEP as input data for determining the SEP or IMFP. The REELS analysis does not require any reference material and can determine the differential SEP (DSEP) describing energy loss probability due to single surface excitation event in addition to SEP or IMFP. However, the REELS analysis also requires the IMFP or SEP as an input data. Recently, a procedure for determining the differential inelastic mean free path (DIMPF) and DSEP from two REELS spectra using the elastic

cross section and an estimate for the IMFP as input parameter [14] has been proposed. The authors have also been involved in the study on the interaction of electrons with solid surface [15-19], and recently proposed an analytical approach to determine simultaneously the IMFP, SEP and DSEP with absolute units from on absolute REELS spectrum [20,21]. The proposed approach requires only the normalized DIMFP and the elastic scattering cross section as input parameters.

With respect to the theoretical approach for studying the interaction of electrons with solid surfaces, theoretical studies based on the dielectric response of solid to external charged particles has been intensively performed [15,22-25]. Another powerful theoretical approach for understanding the interaction of electrons with the solid surface is Monte Carlo (MC) simulation of an electron spectrum. However, most of the MC simulations of electron spectrum do not take into account the surface excitation, and only a few MC simulation codes take it into account [24]. The authors investigated simple modeling of MC simulation of the REELS spectrum by taking into account energy loss processes by surface excitations [26]. In the developed MC simulation, the IMFP, SEP and DSEP determined by the REELS analysis can be used for describing the inelastic interactions of electrons with solids.

In the present paper, the results of the investigation of the inelastic interaction of medium-energy electrons with the Ni surface using the analytical approach proposed by the authors were described. The determined IMFP, SEP, and DSEP are discussed by comparing with those calculated by predictive equations and/or theory. The results of the application of those parameters to the MC simulation of the REELS spectra were also described.

2. Experimental

All experiments were performed using a noble cylindrical mirror analyze (CMA) developed by one of the authors (K.G.) [27]. The CMA equipped with a Faraday cup as a detector, and provides the absolute current of signal electrons. The base pressure of the apparatus was 2×10^{-8} Pa. The sample was a polycrystalline Ni, and its surface was cleaned by sputter cleaning using 250-300 eV Ar^+ ions. The primary energy of electrons for the REELS measurement was varied from 300 to 3000 eV. The beam current was 1 μA. The incident and detection angles of electrons were the surface normal and 42.3±6°. The energy resolution was 0.25%. The transmission function of the CMA used for the correction of the intensity scale of spectra was that estimated by the measurement of the transmission of light [1]. The experimental setup is detailed elsewhere [1].

3. Analytical approach

In the present analytical approach, the IMFP, SEP and DSEP are simultaneously determined from an absolute REELS spectrum. The approach is based on the Landau theory [28] originally describing the energy losses of electrons in solids when the angular deflection of electrons can be neglected. The Landau theory can be extended by taking into account angular deflections of moving electrons by elastic scattering and energy losses by surface excitations, and may be given by [20,21]

$$J(s)=F(s)\sum_{m=0}^{\infty}\alpha_{\mathrm{m}}\left[\lambda_{\mathrm{b}}K_{\mathrm{b}}(s)\right]^{m}\sum_{l=0}^{\infty}P_{\mathrm{s}}^{\mathrm{total},l}\left[K_{\mathrm{s}}^{\mathrm{in}}(s)/P_{\mathrm{s}}^{\mathrm{in}}\right]^{l} \quad (1)$$

where $J(s)$ and $F(s)$ are the Fourier transforms of a measured REELS spectrum $J(E)$ and the energy distribution of primary electrons $F(E)$. s is the Fourier parameter conjugate to the energy E. The first and second Σ terms with respect to the summation over m and l describe the transport of electrons in the bulk and energy loss processes by surface excitations, respectively.

m in the first Σ term is the number of bulk excitation events and α_m describes the probability that electrons participate in m-fold bulk excitation events in solids. λ_{b} is the IMFP and $K_{\mathrm{b}}(s)$ is the Fourier transform of the DIMFP for bulk excitation $K(\Delta E)$, where ΔE is the energy loss. $K(\Delta E)$ satisfies the following relation with λ_{b}

$$1=\lambda_{\mathrm{b}}\int_{0}^{E_{\mathrm{p}}}K_{\mathrm{b}}(\Delta E)\,d(\Delta E) \quad (2)$$

l in the second Σ term is the number of surface excitation events and $P_{\mathrm{s}}^{\mathrm{total},l}$ is the probability that electrons participate in l-fold surface excitation events. Note that $l>2$ is even possible since an electron can participate in surface excitation events more than twice when it cross the surface once [29], though the possibility is very low as confirmed in Fig. 5 below. $P_{\mathrm{s}}^{\mathrm{in}}$ and $K_{\mathrm{s}}^{\mathrm{in}}(s)$ are the SEP and the Fourier transform of the DSEP $K_{\mathrm{s}}^{\mathrm{in}}(\Delta E)$ for incoming electrons. $P_{\mathrm{s}}^{\mathrm{in}}$ and $K_{\mathrm{s}}^{\mathrm{in}}(\Delta E)$ satisfies,

$$1 = \left(P_{\mathrm{s}}^{k}\right)^{-1} \int_{0}^{E_{\mathrm{p}}} K_{\mathrm{s}}^{k}\left(\Delta E\right) d\left(\Delta E\right) \tag{3}$$

$P_{\mathrm{s}}^{\mathrm{total},l}$ is given by

$$P_{\mathrm{s}}^{\mathrm{total},l} = \sum_{l_{\mathrm{in}}=0}^{l} \frac{\left[\Theta\left(\theta_{\mathrm{in}}, \theta_{\mathrm{out}}\right)\right]^{\left(l-l_{\mathrm{in}}\right)} \left(P_{\mathrm{s}}^{\mathrm{in}}\right)^{l}}{l_{\mathrm{in}}!\left(l-l_{\mathrm{in}}\right)!} \times \exp\left\{-\left[1+\Theta\left(\theta_{\mathrm{in}}, \theta_{\mathrm{out}}\right)\right] P_{\mathrm{s}}^{\mathrm{in}}\right\} \tag{4}$$

$$\Theta\left(\theta_{\mathrm{in}}, \theta_{\mathrm{out}}\right) = \cos\theta_{\mathrm{in}} / \cos\theta_{\mathrm{out}} \tag{5}$$

where $l=l_{\mathrm{in}}+l_{\mathrm{out}}$, and l_{in} and l_{out} are the number of surface excitation events undergone by a signal electron on its incoming and outgoing trajectories, respectively. θ_{in} and θ_{out} are the incident and emission angle of the signal electron, respectively.

In the present analysis, a REELS spectrum is self-consistently deconvoluted into components relevant to electrons participating in m-fold bulk (m=0, 1, 2, …) and l-fold surface (l=0, 1, 2, …) excitation events using eq. (1). A REELS spectrum, $J(E)$, is obtained by correcting the intensity of the REELS spectrum using the transmission function. The energy distribution of primary electrons, $F(E)$, is deduced from the elastic peak of the REELS spectrum. The DIMFP, $K(\Delta E)$, is calculated using the dielectric response theory [30] with the Penn's algorithm [31] based on the Ritchie-Howie algorithm [32] for the extension of the ω-dependent energy loss function to the momentum-energy loss space,

$$K_{\mathrm{b}}\left(\Delta E\right) = \frac{1}{2\pi a_0 E_0} \int_{0}^{E_{\mathrm{p}}} \frac{d\left(\hbar\omega_0\right)}{\Delta E\left(\Delta E - \hbar\omega_0\right)} \hbar\omega_0 \times \mathrm{Im}\left[\frac{-1}{\varepsilon\left(\omega_0\right)}\right] \Theta\left[\frac{\hbar^2}{2m}\left(2k\bar{q} - \bar{q}^{2}\right) - \Delta E\right] \tag{6}$$

where a_0 is the Bohr radius, $\Theta(x)$ is the step function representing the lows of momentum and energy conservation. $\hbar\bar{q}$ is the momentum transfer satisfying

$$\Delta E = \hbar\omega_0 + \hbar^2 \bar{q}^{2} / 2m \tag{7}$$

The energy loss function was calculated from optical data [33]. Then, the normalized DIMFP, $\lambda_{\mathrm{b}}K(\Delta E)$, is obtained by multiplying $K(\Delta E)$ by λ_{b}.

For deconvolution procedure, the path-length distribution, $d\eta/dx$, is calculated by MC simulation, in which only the angular deflection by elastic scattering is taken into account (Model I below). Using $d\eta/dx$, α_m is calculated by

$$\alpha_m = \int_{0}^{\infty} \frac{d\eta}{dx} \frac{1}{m!} \left(\frac{x}{\lambda_{\mathrm{b}}}\right)^{m} \exp\left(-\frac{x}{\lambda_{\mathrm{b}}}\right) dx \cdot \tag{8}$$

Using experimentally obtained $J(s)$ and $F(s)$, and calculated $\lambda_{\mathrm{b}}K(\Delta E)$ and α_m, $P_{\mathrm{s}}^{\mathrm{in}}$ and $K_{\mathrm{s}}^{\mathrm{in}}(\Delta E)$ are uniquely determined by deconvolution according to eq. (1). However, $P_{\mathrm{s}}^{\mathrm{in}}$ and $K_{\mathrm{s}}^{\mathrm{in}}(\Delta E)$ obtained at this stage of the analysis does not satisfy the physically defined eq. (3). Therefore, as the next step of the analysis, λ_{b}. is modified, and $P_{\mathrm{s}}^{\mathrm{in}}$ and $K_{\mathrm{s}}^{\mathrm{in}}(\Delta E)$ are deduced again using modified α_m in the same manner. Modifying λ_{b} and deducing $P_{\mathrm{s}}^{\mathrm{in}}$ and $K_{\mathrm{s}}^{\mathrm{in}}(\Delta E)$ are repeated as iterative procedures until the deduced $P_{\mathrm{s}}^{\mathrm{in}}$ and $K_{\mathrm{s}}^{\mathrm{in}}(\Delta E)$ satisfy eq. (3). Finally, λ_{b}, $P_{\mathrm{s}}^{\mathrm{in}}$ and $K_{\mathrm{s}}^{\mathrm{in}}(\Delta E)$ are self-consistently determined. Details of the present absolute REELS analysis and several assumptions made for the theoretical approach are described elsewhere [20,21].

Note that the more detailed transmission function of the CMA has just been reported by one of the authors (K.G.) [34]. The difference in the transmission function between that used in the present study basing on the optical measurement and that more precisely measured using mini electron gun may introduce significant difference in the obtained SEP when the SEP is determined from only the absolute elastic peak intensity [35]. In contrast, the SEP obtained by the present analysis might not be affected significantly since both SEP and IMFP were determined simultaneously and the background of spectra is also used as well as the elastic peak. Further investigation using the newly measured transmission function is underway.

4. Monte Carlo simulation

4.1. Model I (only elastic scattering)

For calculating the path-length distribution, $d\eta/dx$, required for the REELS analysis, the electron trajectories are simulated by taking into account only the elastic scattering as the type of scattering. The step length Λ between two successive elastic collision events is determined by an uniform random number $R_1 \in [0,1]$ within the scheme of the Poisson stochastic process as,

$$\Lambda = -\lambda_{\mathrm{elastic}} \ln\left(R_1\right) \tag{9}$$

where $\lambda_{\mathrm{elastic}}$ is the elastic mean free path.

The scattering angle ϕ is determined by the random number R_2 as

$$R_2 = \frac{\int_0^{\phi} \frac{d\sigma_{\text{elastic}}}{d\phi'} d\phi'}{\int_0^{\pi} \frac{d\sigma_{\text{elastic}}}{d\phi'} d\phi'} \tag{10}$$

where $d\sigma_{\text{elastic}}/d\phi$ is the differential elastic scattering cross section. The elastic mean free path and differential elastic scattering cross section were calculated using Mott cross sections calculated with the partial-wave expansion method using the Thomas-Fermi-Dirac potential [36-38].

4.2. Model II (with inelastic scattering)

In Model II, the inelastic scattering due to both bulk and surface excitations are taken into account as the type of scattering in order to simulate REELS spectra. The step length Λ between two successive collision events in the bulk is determined using eq. (11) instead of (9)

$$\Lambda = -\lambda_{\text{total}} \ln(R_3) \tag{11}$$

where λ_{total} is the total mean free path given by,

$$\lambda_{\text{total}}^{-1} = \lambda_{\text{elastic}}^{-1} + \lambda_{\text{b}}^{-1}. \tag{12}$$

The type of scattering is determined by another random number R_4 as

$$\begin{cases} \textit{elastic}, & \textit{for } R_4 < \lambda_{\text{elastic}}^{-1} / \lambda_{\text{total}}^{-1} \\ \textit{inelastic} & \textit{otherwise} \end{cases}. \tag{13}$$

When the type of scattering is the elastic collision, the scattering angle is determined as that in Model I described above. When the type of scattering is the inelastic collision, the amount of the energy loss ΔE by bulk excitation is determined by

$$R_5 = \frac{\int_0^{\Delta E} \lambda_{\text{b}} K_{\text{b}}(\Delta E') d(\Delta E')}{\int_0^{E_{\text{p}}} \lambda_{\text{b}} K_{\text{b}}(\Delta E') d(\Delta E')}. \tag{14}$$

Details of the MC modeling of REELS spectra, where only bulk excitations are taken into account as inelastic collisions, are described elsewhere [39,40].

In order to describe energy losses by surface excitations in MC simulation, the Poisson stochastic process was assumed. Signal electrons undergo surface excitations when they cross the surface on their incoming and outgoing ways. The numbers of surface excitation events experienced by incident and backscattered electrons crossing the surface on their incoming and outgoing trajectories, L_{in} and L_{out}, respectively, are determined by

$$\frac{\sum_{l=0}^{L_k-1} p_l^k}{\sum_{l=0}^{\infty} p_l^k} < R_6 < \frac{\sum_{l=0}^{L_k} p_l^k}{\sum_{l=0}^{\infty} p_l^k} \tag{15}$$

P_l^k is the probability that the electron participates in l-fold surface excitation events on its incoming (k=in) and outgoing (k=out) trajectories. P_l^k satisfies the relation

$$\sum_{l=0}^{\infty} p_l^k = 1 \tag{16}$$

and expressed using SEP for incoming and outgoing electrons, P_{s}^{in} and $P_{\text{s}}^{\text{out}}$, by

$$p_l^k = \frac{1}{l!}\left(P_s^k\right)^l \exp\left(-P_s^k\right). \tag{17}$$

The amount of the energy loss ΔE by a single surface excitation event is determined using

$$R_7 = \frac{\int_0^{\Delta E} \left(P_{\text{s}}^k\right)^{-1} K_{\text{s}}^k(\Delta E') d(\Delta E')}{\int_0^{E_{\text{p}}} \left(P_{\text{s}}^k\right)^{-1} K_{\text{s}}^k(\Delta E') d(\Delta E')}. \tag{18}$$

Here, P_{s}^{in} and $P_{\text{s}}^{\text{out}}$, and $K_{\text{s}}^{\text{in}}(\Delta E)$ and $K_{\text{s}}^{\text{out}}(\Delta E)$ are assumed to satisfy the relations

$$K_{\text{s}}^{\text{out}}(\Delta E) = \Theta(\theta_{\text{in}}, \theta_{\text{out}}) K_{\text{s}}^{\text{in}}(\Delta E) \tag{19}$$

$$P_{\text{s}}^{\text{out}} = \Theta(\theta_{\text{in}}, \theta_{\text{out}}) P_{\text{s}}^{\text{in}}. \tag{20}$$

In the case of the multiple surface excitation (L_{in}≥2 or L_{out}≥2), the total amount of energy loss due to L_k-fold surface excitation events is calculated by repeating the calculation of eq. (18) L_k times.

In the model II of the MC simulation, the values of the IMFP λ_{b}, SEP P_{s}^k and DSEP K_{s}^k(ΔE), are described by those absolutely determined by the present REELS analysis. During the transport of a signal electron in solids, the mean free path, elastic cross section, DIMFP, SEP and DSEP are changed depending on the kinetic energy of the electron. In the present MC simulation, however, we significantly reduced the calculation time by assuming that the values of those parameters for the certain primary energy can be used during calculating a

REELS spectrum at the corresponding primary energy. As observed later, this is a reasonable assumption since we simulated REELS spectra for the maximum energy loss of 50 to 100 eV depending on the primary energy, which is small enough to regard those parameters to be independent on the kinetic energy of electrons.

5. Results and discussion

Figure 1 shows response functions and their deconvolution into components due to *m*-fold bulk and *l*-fold surface excitations. The response function was obtained by the inverse Fourier transform of $J(s)/F(s)$, which corresponds to the energy loss distribution for one primary electron. It is found that the relative contribution of the components due to surface excitations (s_1 and s_2) is larger than those due to bulk excitations (b_1 and b_2) for the lower primary energy. The energy loss processes in the low-energy loss region near the elastic peak is dominated by surface excitations for low-energy electrons. Note that the lower order components with $m+l\leq 2$, in particular, those due to single surface (s_1, m=0 and l=1) and single bulk (b_1, m=1 and l=0) excitations, form most of the energy loss spectra in the energy loss region of 0-40 eV near the elastic peak, which is important for background subtraction in quantitative analysis.

In Fig. 2, the IMFP determined by the present analysis, λ_b^{pre}, is compared with that calculated by the TPP-2M predictive equation [41], $\lambda_b^{TPP\text{-}2M}$. The plots of the percentage difference of λ_b^{pre} from $\lambda_b^{TPP\text{-}2M}$ calculated by [42]

$$\Delta\lambda_b = \left(\lambda_b^{pre} - \lambda_b^{TPP\text{-}2M}\right)\times 100/\lambda_b^{TPP\text{-}2M} \qquad (21)$$

is also shown. The agreement between λ_b^{pre} and $\lambda_b^{TPP\text{-}2M}$ is found to be fairly good. $\Delta\lambda_b$ is slightly positive at low energies and negative for high energies. For further quantitative comparison of λ_b^{pre} and $\lambda_b^{TPP\text{-}2M}$, the root-mean-square (RMS) difference $\Delta\lambda_b^{RMS}$ was calculated. $\Delta\lambda_b^{RMS}$ is defined as [42]

$$\Delta\lambda_b^{RMS} = \sqrt{\frac{1}{r}\sum_{j=1}^{r}\left(\lambda_b^{pre} - \lambda_b^{TPP\text{-}2M}\right)^2} \qquad (22)$$

where r is the number of IMFP data values, and was calculated to be 3.1 Å,. Thus, $\Delta\lambda_b^{RMS}$ value indicates that the IMFPs deduced from the present absolute analysis agree reasonably well with the theoretical predictions, confirming that the present approach is effective for the experimental determination of IMFPs.

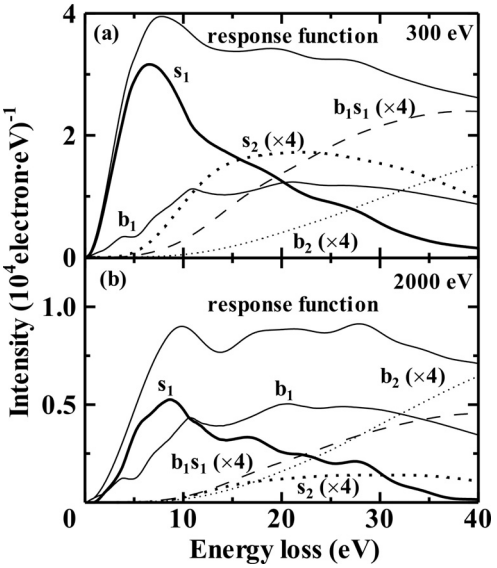

Fig.1. Response functions of REELS spectra for Ni and their deconvolution into components relevant to *m*-fold bulk and *l*-fold surface excitations at primary energies of (a) 300 and (b) 2000 eV. The components satisfying $m+l\leq 2$ are shown. The components corresponding to $m+l=2$ are multiplied by a factor of 4. Single surface excitation (s_1, m=0 and l=1): thick solid line. Single bulk excitation (b_1, m=1 and l=0): thin solid line. Twofold surface excitation (s_2, m=0, l=2): thick dotted line. Twofold bulk excitation (b_2, m=2 and l=0): thin dotted line. Single surface and single bulk excitations (b_1s_1, m=1 and l=1).

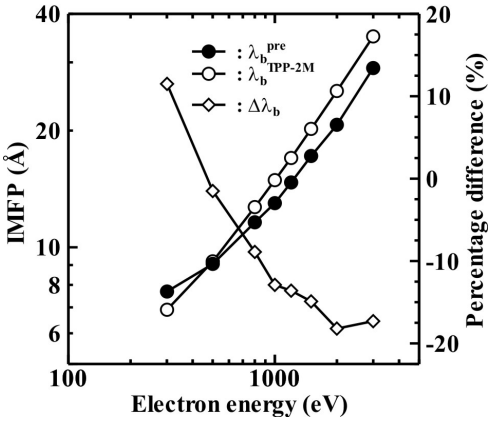

Fig. 2. IMFPs determined by the present analysis λ_b^{pre} (solid circles). Open circles represent the IMFPs calculated using the TPP-2M predictive equation, $\lambda_b^{TPP\text{-}2M}$. $\Delta\lambda_b$ is the percentage difference between the present IMFPs and those calculated using the TPP-2M equation.

Figure 3 shows plots of the SEPs deduced by the present REELS analysis. The present SEPs are fitted with the simple Chen equation [2],

$$P_s = \frac{a}{\sqrt{E}}\left(\frac{1}{\cos\theta_{in}} + \frac{1}{\cos\theta_{out}}\right) \quad (23)$$

This fit gives a=4.3 ($eV^{1/2}$) with an RMS deviation of 0.038, as plotted by the thick solid line. It is found that the present SEPs show reasonable agreement with those calculated using predictive equations of the SEP in Ni reported by Werner [43] and Gergely [44]. Note that plots in Fig. 5 show a slightly complicated dependence on the energy rather than the straight line in log-log plot that expected from the theoretical prediction. For better comparison with other predictive equations and for a more simple formula for the correction, fitting to the simple Chen's equation was performed.

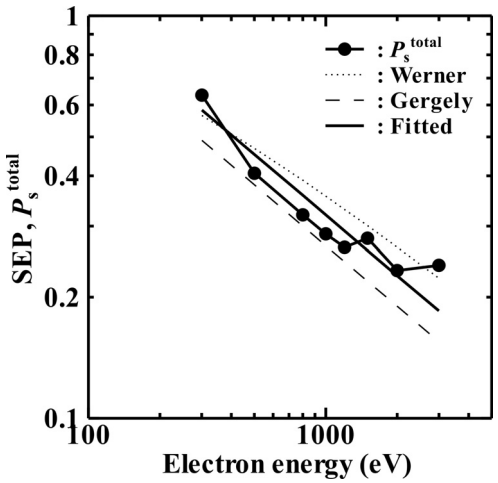

Fig. 3. SEPs deduced by the present analysis. Thin dotted and long dash lines represent the SEPs calculated using Werner's equation [43] and Gergely's equation [44], respectively. The thick solid line shows the fitted curve [eq. (22)].

Figure 4(a) shows the DSEP for incoming electron, the incident angle of which is 0°, obtained by the present analysis for electrons of 300, 800 and 1200 eV. For comparison, the DSEPs theoretically calculated using Tung's model [45] are shown in (b). For the theoretical calculation, the dielectric function modeled by fitting a Drude-Lindhard type of expansion to optical data [45] was used. The fitting parameters for Ni are listed in the literature [21]. The DIMFPs, the intensity of which, i.e., the IMFP, was determined by the present study, are also shown in (c). A comparison between (a) and (b) reveals that the present DSEP shows the fairly good overall agreement with the theoretical prediction. In both figures, the most probable energy loss by single surface excitation is found to be approximately 7.5 eV. A comparison between (b) and (c) indicates the energy loss processes in the low-energy loss region is dominated by surface excitations. Differences between the present DSEPs and theoretical results are observed for energy losses larger than 15 eV. This might be due to the deficiencies in the optical data used for the calculation of the normalized DIMFP and for parameterization of the model dielectric function [21].

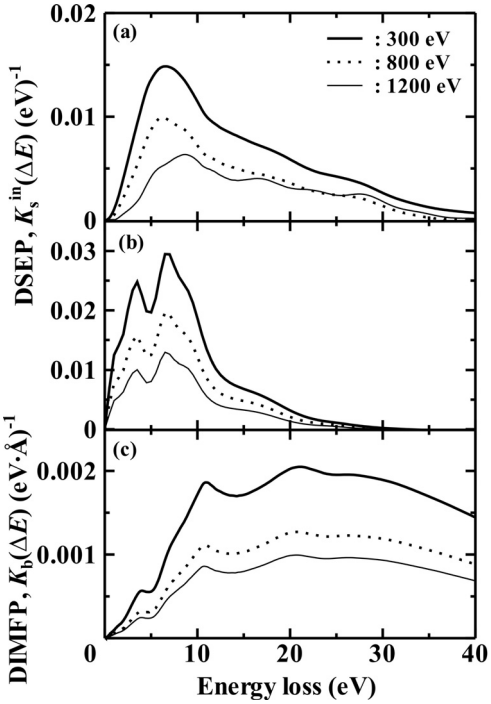

Fig. 4. (a) DSPEs obtained by the present study. (b) DSEPs calculated using Tung's model [45]. (c) DIMFPs determined in the present study. The primary energy of electrons are 300, 800 and 1200 eV.

Figures 5(a) and (b) show the probability $\alpha_m P_s^{total,l}$ of primary electrons of 300 and 2000 eV participating in *m*-fold bulk and *l*-fold surface excitations in the present REELS measurement. The contribution of multiple surface excitation events ($l \geq 2$) is higher for the lower primary energy. The contribution of twofold surface excitation events is ~20% of that of l=0 for 300 eV, and decreases to only a few % for 2000 eV. These results indi-

cate that the contribution of surface excitations strongly depends on the energy of signal electrons. This primary energy dependence reveals that care concerning surface excitations is required for the improvement of the accuracy of quantification using surface electron spectroscopy.

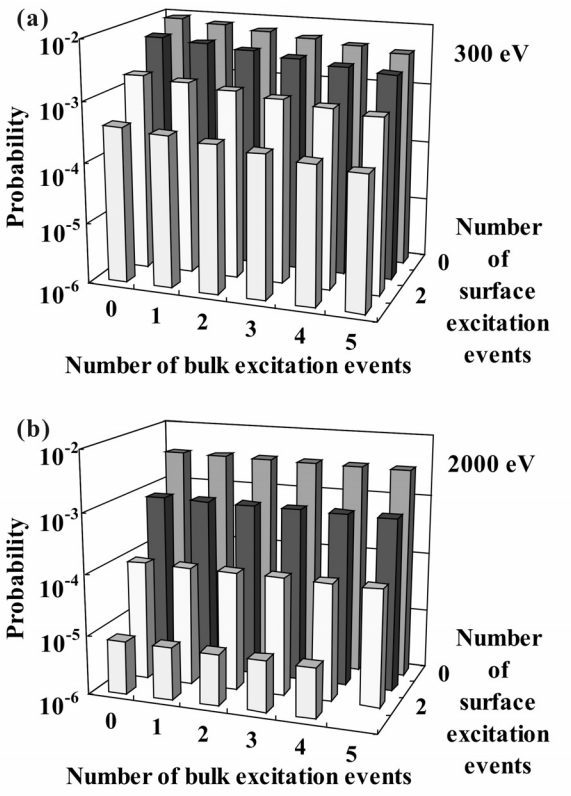

Fig. 5. Probability of electrons participating in *m*-fold bulk and *l*-fold surface excitation events in the present REELS measurement. The primary energy of electrons are (a) 300, (b) 2000 eV, respectively.

Figure 6 shows the REELS spectra calculated using the present MC simulation with Model II, where energy losses by surface excitations are taken into account. For comparison, the experimental spectra and those simulated without taking into account surface excitations are shown. It is confirmed that the present MC simulation with Model II reproduces the absolute intensity of both the elastic peak and the background very well without any fitting parameters. The same degree of the agreement was observed for all other REELS spectra obtained at different primary energies. In contrast, the MC simulation without surface excitations significantly overestimates the elastic peak intensity. The background intensity near the elastic peak, where contribution of energy losses by surface excitations is significant, are underestimated. These results suggest that quantitatively understanding of AES and XPS spectra requires information on energy loss processes due to surface excitations in the energy loss region near the elastic peak.

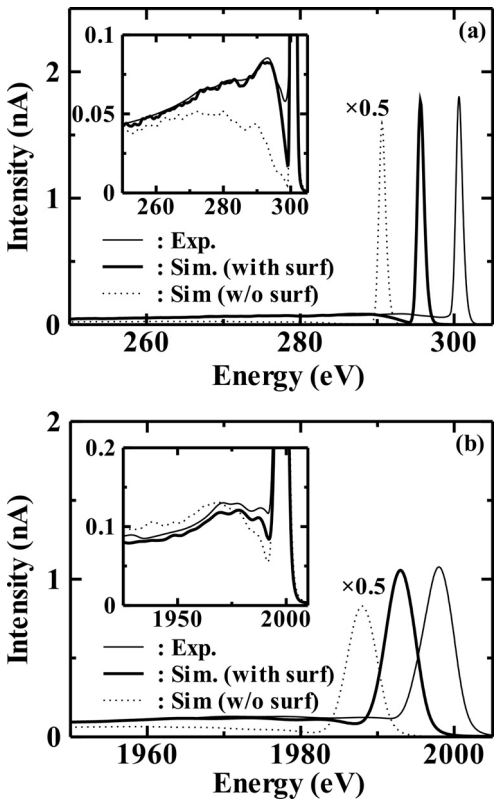

Fig. 6. REELS spectra simulated by MC simulation, in which energy loss processes by surface excitation is taken into account (thick solid line). The primary energies of electrons are (a) 300 and (b) 2000 eV. Thin solid line shows the experimental absolute REELS spectra. Dotted line represents the simulated spectra without taking into account surface excitations. The experimental spectra and spectra simulated without surface excitation were shifted towards the lower energy side for better comparison. The spectra simulated without surface excitations are multiplied by the factor of 0.5 for better comparison of the overestimated elastic peak intensity. Insets show the background of the spectra on an enlarged scale.

Note that the simulated spectra tend to underestimate the intensity of the background at the tail of the elastic peak at the lower energy side. This tendency is significant for the lower primary energy. This is attributed to the uncertainty in the elastic peak profile. The higher the primary energy is, the smaller the underestimation is,

since fine loss structures are smeared out at higher primary energies because of the lower energy resolution. It should be noted that the underestimation of the elastic peak intensity observed in Fig. 5(a) is less than 1%, causing almost no error in quantification.

6. Summary

The analytical approach to deduce the IMFP, SEP and DSEP from an absolute REELS spectrum and the results of the analysis are outlined. The results of the application of the obtained IMFP, SEP and DSEP to MC simulation of REELS spectra are also described. The present approach is one of the powerful approaches to experimentally determine absolutely the IMFP, SEP and DSEP for medium-energy electrons. The investigation of the REELS spectra by MC simulation is also effective to understand the interaction of medium-energy electrons with solid surface. Further investigation using the present analytical approach with the newly measured transmission function [34] is underway.

7. References

[1] S. Tanuma, S. Ichimura, and K. Goto K, *Surf. Interface Anal.* **30**, 212 (2000).
[2] Y. F. Chen, *Surf. Sci.* **519**, 115 (2002).
[3] J. Zemek, P. Jiricek, B. Lesiak, and A. Jablonski, *Surf. Sci.* **531**, L335 (2003).
[4] G. Gergely, M. Menyhard, S. Gurban, J. Toth, and D. Varga, *Surf. Interface Anal.* **36**, 1098 (2004).
[5] G. Gergely, M. Menyhard, S. Gurban, J. Toth, and D. Varga, *Surf. Interface Anal.* **36**, 1098 (2004).
[6] S. Gurban, G. Gergely, J. Toth, D. Varga, A. Jablonski, and M. Menyhard, *Surf. Interface Anal.* **38**, 624 (2006).
[7] W. S. M. Werner, W. Smekal, C. Tomastik, and H. Störi, *Surf. Sci.* **486**, L461 (2001).
[8] W. S. M. Werner, *Surf. Sci.* **526**, L159 (2003).
[9] W. S. M. Werner, *Surf. Interface Anal.* **35**, 347 (2003).
[10] W. S. M. Werner, L. Köver, S. Egri, J. Tóth, and D. Varga, *Surf. Sci.* **585**, 85 (2005).
[11] G. Gergely, M. Menyhard, S. Gurban, A. Sulyok, J. Toth, D. Varga, and S. Tougaard, *Solid State Ionics* **141-142**, 47 82001).
[12] G. Gergely, M. Menyhard, S. Gurban, A. Sulyok, J. Toth, D. Varga, S. Tougaard, *Surf. Interface Anal.* **33**, 410 (2002).
[13] S. Gurban, G. Gergely, M. Menyhard, J. Adam, A. Adamik, Cs. Daroczi, J. Toth, D. Varga, A. Csik, and S. Tougaard, *Surf. Interface Anal.* **34**, 206 (2002).
[14] W. S. M. Werner, *Phys. Rev. B* **74**, 075421 (2006).
[15] T. Nagatomi, R. Shimizu, and R. H. Ritchie, *Surf. Sci.***419**, 158 (1999).
[16] T. Nagatomi, Z. J. Ding, and R. Shimizu, *Surf. Sci.* **359**, 163 (1996).
[17] T. Nagatomi, T. Kawano, H. Fujii, E. Kusumoto, and R. Shimizu, *Surf. Sci.* **416**, 184 (1998).
[18] T. Nagatomi, T. Kawano, and R. Shimizu, *J. Appl. Phys.***83**, 8016 (1998).
[19] T. Nagatomi, R. Shimizu, and R. H. Ritchie, *J. Appl. Phys.* **85**, 4231 (1999).
[20] T. Nagatomi and K. Goto, *Appl. Phys. Lett.* **87**, 224107 (2005).
[21] T. Nagatomi and K. Goto, *Phys. Rev. B* **75**, 235425 (2007).
[22] Y. F. Chen and Y. T. Chen, *Phys. Rev. B* **53**, 4980 (1996).
[23] C. M. Kwei, C. Y. Wang, and C. J. Tung, *Surf. Interface Anal.* **26**, 682 (1998).
[24] Z. J. Ding, H. M. Li, Q. R. Pu, Z. M. Zhang, and R. Shimizu, *Phys. Rev. B* **66**, 085411 (2002).
[25] F. Yubero and S. Tougaard, *Phys. Rev. B* **71**, 045414 (2005).
[26] T. Nagatomi and K. Goto, *Surf. Interface Anal.* (*submitted*).
[27] K. Goto, N. Sakakibara, and Y Sakai,. *Microbeam Anal.* **2**, 123 (1993).
[28] L. Landau, *J. Phys. (Moscow)* **8**, 201 (1944).
[29] T. Nagatomi and K. Goto, *J. Surf. Anal.* **13**, 212 (2006) (*in Japanese*).
[30] D. Pines, *Elementary Excitations in Solids* (W. A. Benjamin, New York, 1964).
[31] D. R. Penn, *Phys. Rev. B* **35**, 482 (1987).
[32] R. H. Ritchie and A. Howie, *Phil. Mag.* **36**, 463 (1977).
[33] E. D. Palik, *Handbook of Optical Constants of Solids* (Academic, New York, 1985).
[34] A. Alkafri, Y. Ichikawa, R. Shimizu, and K. Goto, *J. Surf. Anal.* **14**, 2 (2007).
[35] S. Tanuma, H. Yoshikawa, N. Okamoto, and K. Goto, 12th European Conference on Application of

Surface and Interface Analysis (ECASIA'07), QUA-1070-01 (2007).

[36] N. F. Mott and H. S. W. Massey. *The Theory of Atomic Collisions* (Oxford, London, 1965) 6th ed.

[37] Y. Yamazaki, Ph.D Thesis, Osaka University, 1977.

[38] S. Ichimura and R. Shimizu, *Surf. Sci.* **112**, 386 (1981).

[39] Z. J. Ding and R. Shimizu, *Surf. Sci.* **222**, 313 (1989).

[40] Z. J. Ding, Ph.D Thesis, Osaka University, 1990.

[41] S. Tanuma, C. J. Powell, and D. R. Penn, *Surf. Interface Anal.* **21**, 165 (1994).

[42] C. J. Powell and A. Jablonski, *J. Phys. Chem. Ref. Data* **28**, 19 (1999).

[43] W. S. M. Werner, L. Köver, S. Egri, J. Tóth, and D. Varga, *Surf. Sci.* **585**, 85 (2005).

[44] G. Gergely, M. Menyhard, S. Gurban, J. Toth, and D. Varga, *Surf. Interface Anal.* **36**, 1098 (2004).

[45] C. J. Tung, Y. F. Chen, C. M. Kwei, and T. L. Chou, *Phys. Rev. B* **49**, 16684 (1994).